# Photophysics of Soret-Excited Tetrapyrroles in Solution. IV. Radiationless Decay and Triplet−Triplet Annihilation Investigated Using Tetraphenylporphinato Sn(IV)

**Manisankar Maiti, Brook R. Danger, and Ronald P. Steer***

*Department of Chemistry, University of Saskatchewan, 110 Science Place, Saskatoon, SK S7N 5C9, Canada*

*Received: July 22, 2009; Revised Manuscript Received: September 3, 2009*

The $S_2$ population decay rates and triplet−triplet annihilation efficiencies of Sn(IV)$Cl_2$TPP have been measured in fluid solutions using its weak $S_2-S_0$ fluorescence as a metric. A detailed description of the excited-state photophysics of Sn(IV)$Cl_2$TPP has allowed comparisons to be made between this rigid, $D_{4h}$ axially coordinated molecule and axially uncoordinated tetrapyrroles of greater flexibility and lower symmetry. $S_2-S_1$ internal conversion is the major $S_2$ population decay path for Sn(IV)$Cl_2$TPP as it is for the $S_2$ states of all other $d^0$ and $d^{10}$ metalated tetrapyrroles. The $S_2$ state of Sn(IV)$Cl_2$TPP exhibits $S_2-S_1$ relaxation rates that follow the energy gap law of radiationless transition theory and are only slightly faster than those exhibited by MgTPP and the weak coupling limit. Differences in $S_2-S_1$ radiationless decay rates among the series MTPP (M = Mg, Zn, Cd, $SnCl_2$) cannot be traced to differences in the displacements of the $S_2$ and $S_1$ potential surfaces. Instead, the most likely source of the large differences in $S_2-S_1$ radiationless decay rates between CdTPP and Sn(IV)$Cl_2$TPP is the lower symmetry of the former (near $C_{4v}$), which permits a much larger number of vibrations to participate in $S_2-S_1$ vibronic coupling. Triplet−triplet annihilation of the type $2T_1 \rightarrow S_2 + S_0$ has been observed in Sn(IV)$Cl_2$TPP for the first time, but is of substantially lower efficiency than seen in ZnTPP in noncoordinating solvents because of its shorter triplet lifetime and the shielding effects of its axial Cl ligands, which tend to block the short-range interaction needed for Dexter energy transfer.

## Introduction

Metalloporphyrins and other metalated tetrapyrroles are ubiquitous in nature[1] and have found increasing use in photon-actuated applications such as oxygen sensors,[2] agents for photodynamic therapy,[3] photonic and molecular logic devices,[4] and dye-sensitized solar cells.[5] Extensive literature on the spectroscopy and kinetics of the lowest excited singlet ($S_1$) and triplet ($T_1$) states of these compounds supports these applications.[6] However, relatively little is known about the photophysics of the higher excited states ($S_n$, $n > 1$)[7] that can be populated via one-photon excitation in the Soret and higher energy absorption bands, via multiphoton excitation at similar total absorbed photon energies, or via excited state annihilation. This paucity of photophysical data concerning highly excited valence states of polyatomic molecules is not confined to the tetrapyrroles and has been noted previously by those designing molecular logic and other devices based on a variety of chromophores.[4] Given this situation and, specifically, the growing importance of more highly excited states in designing dye-sensitized solar cells using noncoherent photon upconversion processes,[8] this information deficit should be considered serious and in urgent need of remediation.

We have sought to fill this information gap via a series of papers exploring the photophysics of the higher singlet states of metalated tetrapyrroles in solution[9−12] and in thin films.[13] The rates of population decay of the excited singlet states (labeled $S_2$ here) produced on one-photon excitation in the Soret bands of these compounds are determined almost exclusively by their rates of radiationless decay. Using steady-state and femtosecond time-resolved fluorescence data, we have made considerable progress in quantifying the structure−property relationships governing these radiationless processes. In summary, using a time-dependent perturbation theory-based analysis of the $S_2$ population decay rates of magnesium, zinc, and cadmium tetraphenylporphyrin (MTPP, M = Mg, Zn, Cd), of a series of eight other zinc porphyrins of varying structure, and of two metallocorroles, we have come to the following general conclusions: (i) Tetrapyrroles that coordinate $d^0$ or $d^{10}$ metal ions exhibit $S_2$ radiationless decay mainly by $S_2-S_1$ internal conversion; complications due to charge transfer and d,d excited states characteristic of metals with unfilled d shells are avoided.[9,10] (ii) Of all of the tetrapyrroles metalated with $d^0$ and $d^{10}$ ions investigated to date, only MgTPP exhibits radiationless decay characteristic of the weak coupling, statistical limit of radiationless transition theory.[9] For MgTPP, the quantum efficiency of $S_2-S_1$ internal conversion is 1.00, and the variation of the rate of this process with the electronic energy gap, $\Delta E(S_2-S_1)$, is determined by the variation in the corresponding Franck−Condon factors, in keeping with the energy gap law. All other metalated tetrapyrroles investigated to date exhibit $S_2-S_1$ population decay rates that are faster than those predicted by the weak coupling limit.[10] (iii) For at least those molecules adequately represented by the $D_{4h}$ point group, in-plane C−C and C−N stretching vibrations are the main accepting modes in the radiationless decay; unlike many other systems, high frequency C−H vibrations play no significant role.[10] (iv) In the tetrapyrroles metalated with heavier atoms (e.g., Cd), $S_2-T_n$ ($n > 2$), intersystem crossing may play a minor role as a parallel radiationless decay route, but does not account for the large differences in the measured $S_2$ population decay rates of these compounds.[9] (v) In the absence of data illuminating other factors that control the $S_2-S_1$ radiationless decay rate, the contribution to these decay rates in excess of the lower limit set by weak vibronic coupling has been attributed empirically[9] to increases

* Corresponding author. Tel.: (306) 966-4667. Fax: (306) 966-4730. E-mail: ron.steer@usask.ca.

10.1021/jp906966h CCC: $40.75 
Published on Web 09/24/2009

in the $S_2-S_1$ interstate coupling energy, $\beta_{el}$. However, other than the Franck−Condon factor's variation with $\Delta E(S_2-S_1)$, the quantities that control the magnitude of the radiationless decay rates have not yet been deduced from analyses of the data available to date and remain largely unknown.

The present Article addresses this deficit in our knowledge of these tetrapyrrolic systems. We report new data characterizing the photophysical behavior of the $S_2$ state of Sn(IV)$Cl_2$TPP in several solvents and show that axially ligated metalloporphyrins such as this are relatively poor candidates for use in photon upconversion schemes based on triplet−triplet annihilation. This porphyrin has a well-established coordination chemistry.[14] Of crucial importance in the present study, it has a rigid $D_{4h}$ structure,[15] so comparisons of its photophysical properties with those obtained previously for other $d^0$ and $d^{10}$ metalated tetrapyrroles with more flexible, average $D_{4h}$ structures or with structures of lower symmetry provide further insight into the role that excited-state potential surface displacements and deformations play in determining the $S_2$ state radiationless relaxation rates of these important compounds.

## Experimental Section

**Materials.** Sn(IV)$Cl_2$TPP was obtained from Porphyrin Systems and contained significant amounts of the corresponding chlorin as an impurity, which was removed by column chromatography on basic alumina. The chlorin is a common porphyrin contaminant and is particularly difficult to remove permanently in the Sn(IV)$Cl_2$TPP system because it can be reformed by photochemical means if trace reductants are present.[16] Fortunately, the absorption and emission spectra of the tin porphyrin and chlorin are sufficiently different that it is possible to choose excitation and emission wavelengths at which the contamination of the porphyrin spectra by the chlorin is all but eliminated (cf., following spectra). Unfortunately, even in the relatively recent literature, the features due to the chlorin contaminant have not always been recognized, leading to serious errors in data interpretation in some papers.[17]

Solvents (Aldrich) were of the highest purity available and were treated with dried molecular sieves to remove traces of water that can act as a chlorine ligand replacement in this system. All experiments were carried out in aerated solutions at room temperature.

**Instrumentation.** The fluorescence upconversion setup used for this work has been described in detail elsewhere.[9] Briefly, a Ti:sapphire femtosecond laser (Coherent, Vitesse Duo) and a regenerative amplifier (Coherent, RegA 9000), operating at a repetition rate of 100 kHz with an output power 330−400 mW at 800 nm and with a 170 to 200 fs fwhm Gaussian cross-correlation trace, were used as the excitation and gate source. The 800 nm output was passed through a 80/20 beam splitter, and the smaller fraction was frequency doubled to produce 400 nm excitation pulses. The larger fraction passed through a stepped variable delay line ($\Delta t \geq 3.3$ fs/step) and was used to upconvert the fluorescence from the sample in a BBO crystal. The upconversion signal was then focused onto the slit of a monochromator (CM112) and detected by a photomultiplier (Hamamatsu, H7732P-01) connected to a two-channel gated photon counter (Stanford Research Systems, SR400) via a preamplifier (Stanford, SR445).

**Methods.** All kinetic data obtained by fluorescence upconversion were analyzed by iterative reconvolution of trial fitting functions with a Gaussian instrumental response function and assessing the goodness-of-fit by examining the magnitude and distribution of residuals. Temporal $S_2$ fluorescence decays were all fit satisfactorily with single exponential decay functions and were independent of solute concentration in the 25−250 $\mu$M range (in ethanol). Temporal $S_1$ fluorescence profiles were fit with a two-component function that accounted for picosecond $S_1$ population rise and nanosecond $S_1$ population decay.

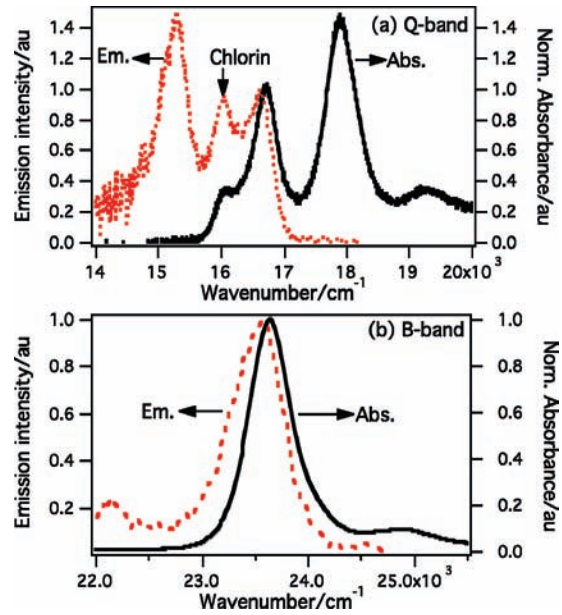


**Figure 1.** Absorption (solid black lines) and emission (broken red lines) spectra of Sn(IV)$Cl_2$TPP in ethanol for (a) the Q-band and (b) the Soret or B-band, with excitation wavelength at 25 000 cm$^{-1}$ (400 nm) in both cases. All spectra have been normalized to the maxima of the 0−0 bands.

Steady-state absorption spectra of Sn(IV)$Cl_2$TPP in various solvents were measured with a Varian-Cary 500 spectrophotometer, and fluorescence spectra were measured by using a Photon Technology International QuantaMaster spectrofluorometer fitted with double monochromators on both the excitation and the emission arms and a calibrated photodiode for correcting the excitation spectra. Care was taken to collect the spectra under the conditions where the detectors were working in the linear response region. All measurements were carried out under identical conditions, keeping excitation and emission slits at 1 mm ($\Delta\lambda = 2.0$ nm). Collection and correction of the emission spectra and processing of the data were done by using the protocol published earlier.[10] Fluorescence quantum yields and internal conversion quantum efficiencies were determined as described previously[9,10] using ZnTPP in ethanol as a reference,[18] and were corrected for small contributions due to chlorin. Triplet−triplet annihilation experiments were performed using the $TEM_{00}$ cw output of a frequency-doubled Nd:YAG laser at 532 nm as the excitation source and an in-house modified SPEX Fluorolog spectrofluorometer for detection. Samples, degassed by several freeze−pump−thaw cycles, were front-face illuminated in an evacuable, triangular cell. Details have been given elsewhere.[12] TTA spectra were collected at several different emission slit widths to obtain good signal-to-noise, and the intensities were scaled to those that would be obtained at the same slit width using an intensity−slit width calibration.

## Results

The absorption and fluorescence emission spectra of Sn(IV)-$Cl_2$TPP were measured in several aerated solvents at room temperature. Those taken in ethanol are shown in Figure 1, and the corresponding fluorescence excitation spectra are shown in

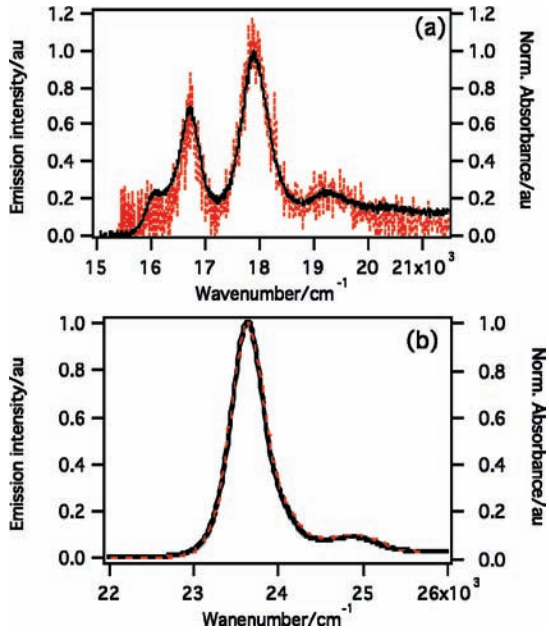


**Figure 2.** Normalized (a) $S_1-S_0$ and (b) $S_2-S_0$ absorption spectra (solid black lines) and emission excitation spectra (broken red lines) of $Sn(IV)Cl_2TPP$ in ethanol obtained by observing $S_1-S_0$ emission at 15 150 $cm^{-1}$ (660 nm).

Figure 2. Note that the feature in the absorption spectrum at ca. 620 nm due to the tin chlorin[17,19] is absent in the fluorescence excitation spectra obtained by monitoring $S_1$ fluorescence at 660 nm and scanning through both the $S_1-S_0$ (Q-band) and the $S_2-S_0$ (Soret or B-band) absorption regions. With the chorin removed, the absorption and Q-band emission spectra are in all respects similar to the spectra of $SnCl_2TPP$ published previously;[17-19] the Soret band emission spectra are new.[20] The corresponding radiative processes are assigned to the $1(^1E_u)-1(^1A_{1\,g})$ and $2(^1E_u)-1(^1A_{1\,g})$ ($S_1-S_0$ and $S_2-S_0$) transitions, respectively; that is, the assignments are the same as those found in all other $D_{4h}$ metalloporphyrins complexed with $d^0$ and $d^{10}$ metal ions.[21]

Note the characteristic strong absorption band in the Soret region and the weaker feature lying about 1350 $cm^{-1}$ further to the blue. Previous time-dependent density functional theory (TD-DFT) calculations[22] have suggested that the Soret bands of common metalloporphyrins could be a composite of two radiative transitions with nonzero oscillator strength and that the weak feature to the blue may be a transition to a separate electronic state (sometimes identified as $3(^1E_u)$). However, very recent calculations based on the MCD spectra[23] now suggest that these two bands are associated with a single electronic transition, $2(^1E_u)-1(^1A_{1\,g})$, and that the weaker feature to the blue is the envelope of a weakly Franck−Condon active set of in-plane $a_{1g}$ ring-stretching vibrations. The features of the Soret emission spectra of all of the $D_{4h}$ MTPP (M = Mg, Zn, $SnCl_2$) molecules[9,10] support this view. The corrected emission spectrum of $Sn(IV)Cl_2TPP$ is an exact mirror image of the corresponding absorption spectrum; the weak feature to the red is located ca. 1400 $cm^{-1}$ from the main band, consistent with Franck−Condon activity in the same set of $a_{1g}$ vibrations in the ground state. The Stokes shifts are small (ca. 100 $cm^{-1}$), in both the B- and the Q-band systems, consistent with the rigid nature of the macrocyclic structure.[15] Note also that the normalized fluorescence excitation spectrum, taken by scanning in the Soret region and observing emission in the strong Q-band feature at 660 nm, reproduces the corresponding absorption spectrum perfectly within experimental error. No excitation wavelength-dependent photophysical process is evident in these steady-state spectra of $Sn(IV)Cl_2TPP$.

Quantum yields of both $S_2-S_0$ and $S_1-S_0$ fluorescence were measured for $Sn(IV)Cl_2TPP$ in a variety of solvents using the well-established corresponding fluorescence yields of ZnTPP as a standard.[18] The data are collected in Table 1. The quantum yield of $S_2-S_0$ fluorescence obtained when exciting $Sn(IV)Cl_2TPP$ in ethanol at 400 nm, $\phi_{fS2} = 7.6 \times 10^{-4}$, is typical. Using this datum and a value of the $S_2-S_0$ radiative rate constant, $k_r = 3.8 \times 10^8\ s^{-1}$ calculated from the Soret band oscillator strength,[24] the population decay time of the $S_2$ state, $\tau_{S2} = \phi_{fS2}/k_r$, is then estimated to be ca. 2.0 ps, in very good agreement with the measured value of 1.9 ps (vide infra). Quantum yields of $S_1-S_0$ fluorescence, $\phi_{fS1}$, have been measured previously by others;[25,26] values of 0.011 in MTHF at room temperature and 0.025 at 77 K and 0.014−0.021 in water−methanol solutions agree reasonably well with those obtained here. We have previously shown[9] that accurate quantum efficiencies of $S_2-S_1$ internal conversion, $\eta_{S2S1}$, can be obtained in these systems by measuring the ratio of the Q-band fluorescence intensity when exciting in the Soret band as compared to that found when exciting in the Q-band (and correcting for absorbed intensity). Applying this technique to $Sn(IV)Cl_2TPP$ in ethanol yields a value of $\eta_{S2S1} = 0.86 \pm 0.05$, close to 1.0 and similar to the values found in many other $d^0$ and $d^{10}$ metalated tetrapyrroles. (Note, however, that $\eta_{S2S1} = 1.00$ for MgTPP.[9])

The electronic energies, $E^{0-0}$, of the $S_2$ and $S_1$ states were obtained from the wavenumber of overlap of the absorption and the corrected normalized emission spectra in the Soret and Q-band regions, respectively. These data are also collected in Table 1. The linear relationship between $\Delta E(S_2-S_1)$ and the Lorenz−Lorentz solvent polarizability function, $f_1 = (n^2 - 1)/(n^2 + 2)$, for $Sn(IV)Cl_2TPP$ is shown in Figure 3 and is similar to those obtained previously for MgTPP and ZnTPP.[9,10] The gradients of such plots, $g = \partial(\Delta E)/\partial(f_1)$, are determined primarily by the difference in the polarizabilities of the $S_2$ and $S_1$ states of the metalloporphyrin and have magnitudes that are proportional to the number of $\pi$ electrons in the molecule's macrocycle (but not in the pendant phenyl groups).[10] An average value of $|g| = (3.6 \pm 0.2) \times 10^3$ cm has been obtained previously for MgTPP, ZnTPP, and several other zinc metalloporphyrins with the same 26 $\pi$ electron macrocycle.[10] The value of $|g| = (3.2 \pm 0.2) \times 10^3$ cm for $Sn(IV)Cl_2TPP$ (Figure 3) is similar to, but slightly smaller than, this average. We speculate that the small difference could be due to the restricted ability of solvent molecules to approach the macrocycle $\pi$ electron system due to the physical shielding effect of the axial chloride ligands, an effect absent in the magnesium- and zinc-containing systems. We can also conclude that, although the chlorine atoms themselves will contribute to the overall polarizability of the $Sn(IV)Cl_2TPP$ molecule, they must do so to the same extent in the two excited singlet states. That is, as noted previously for the substituent phenyl groups,[9,10] the Cl atoms contribute nothing to the differences in the $S_2$ and $S_1$ state polarizabilities, differences that are due almost exclusively to the number of $\pi$ electrons in the macrocycle.

The $S_2$ population decay times were measured for $Sn(IV)Cl_2TPP$ in the same set of solvents (except for $CS_2$) used to obtain quantum yield and spectroscopic data. A typical temporal $S_2$ fluorescence decay profile is shown in Figure 4. The full set of data is summarized in Table 1. The measured $S_2$ population decay times are in the 1−2 ps range, in near perfect agreement

**TABLE 1: Steady-State and Time-Resolved Data for *meso*-Tetraphenylporphinato Tin(IV) Dichloride**

| | | steady-state data[a] | | | | | | |
|---|---|---|---|---|---|---|---|---|
| | | | | | quantum yields | | lifetimes[b] | |
| solvents | $f_1$ | $E^{0-0}(S_2)$ ($cm^{-1}$) | $E^{0-0}(S_1)$ ($cm^{-1}$) | $\Delta E(S_2-S_1)$ ($cm^{-1}$) | $S_2-S_0$ (B-band) | $S_1-S_0$ (Q-band) | $\tau_d(S_2)$ (ps) | $\tau_r(S_1)$ (ps) |
| methanol | 0.203 | 23 710 | 16 735 | 6975 | 0.00065 | 0.022 | 1.79 | |
| ethanol | 0.221 | 23 610 | 16 665 | 6945 | 0.00076 | 0.032 | 1.88 | 1.84 |
| 1-propanol | 0.235 | 23 540 | 16 680 | 6860 | 0.00043 | 0.031 | 1.27 | |
| 1-butanol | 0.242 | 23 500 | 16 650 | 6850 | 0.00053 | 0.038 | 1.31 | |
| THF | 0.246 | 23 410 | 16 585 | 6825 | 0.00086 | 0.018 | 1.71 | |
| DMF | 0.259 | 23 340 | 16 570 | 6770 | 0.00063 | 0.021 | 1.53 | 1.39 |
| toluene | 0.293 | 23 270 | 16 540 | 6730 | 0.00084 | 0.024 | 1.41 | 1.40 |
| benzene | 0.295 | 23 255 | 16 555 | 6700 | 0.00090 | 0.027 | 1.41 | |
| $CS_2$ | 0.355 | 22 870 | 19 390 | 6480 | n.d. | n.d. | | |
| CdTPP in ethanol[c] | 0.221 | 23 160 | 16 280 | 6880 | 0.00014 | | 0.31 | 0.30 |

[a] Wavenumbers are ±10 $cm^{-1}$; $\Delta E$ is ±20 $cm^{-1}$. Quantum yields are ±5%. [b] Averaged over replicate trials; decay constants are ±0.05 ps, and rise times are ±0.07 ps. [c] Data from ref 9.

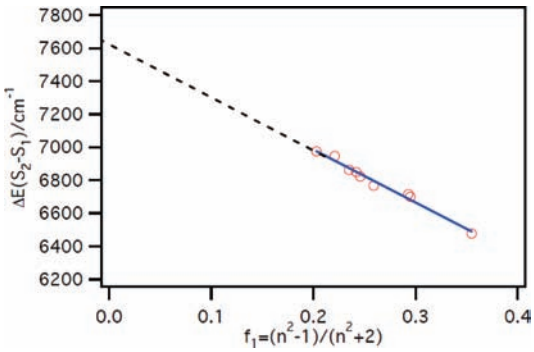


**Figure 3.** $S_2-S_1$ electronic energy gap of Sn(IV)$Cl_2$TPP as a function of the Lorenz−Lorentz polarizability function of the solvent $f_1 = (n^2 - 1)/(n^2 + 2)$. Extrapolation to $f_1 = 0$ gives the energy gap of the bare molecule, 7627 ± 44 $cm^{-1}$. Gradient $g = -(3.2 \pm 0.2) \times 10^3$ cm (see text for significance).

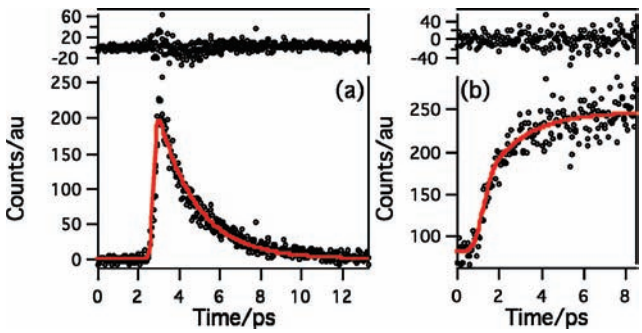


**Figure 4.** (a) $S_2$ fluorescence decay ($\lambda_{em}$ = 433 nm, $\tau_{decay}$ = 1.86 ± 0.03 ps) and (b) $S_1$ fluorescence rise ($\lambda_{em}$ = 654 nm, $\tau_{rise}$ = 1.84 ± 0.23 ps) profiles of Sn(IV)$Cl_2$TPP in ethanol ($\lambda_{ex}$ = 400 nm). The residuals are shown in the top of each panel.

with the estimates provided from the measured fluorescence quantum yield and calculated radiative rate constant data (vide supra). The corresponding nonradiative rate constants, $k_{nr} = (1 - \phi_{fS2})/\tau_{S2} \sim 1/\tau_{S2}$, show the expected general trend with $\Delta E(S_2-S_1)$, and the applicable energy gap law plot is shown in Figure 5, together with the data for MgTPP, ZnTPP, and CdTPP obtained previously.[9] For Sn(IV)$Cl_2$TPP, the energy gap law slope of $-(3.5 \pm 2.2) \times 10^{-4}$ cm and intercept of $10^{14.2\pm1.5}$ $s^{-1}$ are similar to those found for MgTPP[9] and other molecules such as azulene[27] that possess vibronically coupled $S_2$ and $S_1$ states of ($\pi,\pi^*$) character and that conform to the weak vibronic coupling limit.[28] Unfortunately, the lifetime data for Sn(IV)$Cl_2$TPP are not sufficiently accurate and the 275 $cm^{-1}$ span in the values of $\Delta E(S_2-S_1)$ too small to obtain better than

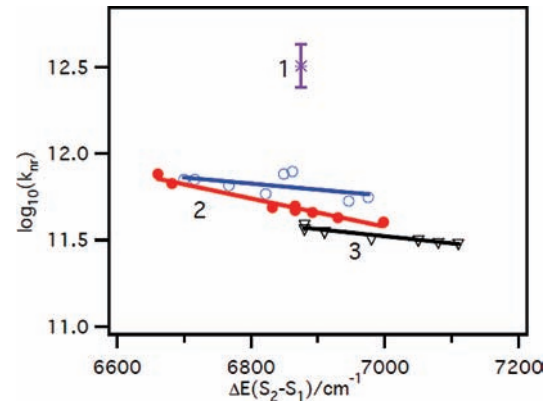


**Figure 5.** Energy gap law plot for Sn(IV)$Cl_2$TPP (blue, ○) assuming $S_2-S_1$ internal conversion is the sole $S_2$ radiationless decay process. Comparable data for (1) CdTPP (violet), (2) ZnTPP (red, ●), and (3) MgTPP (black, ▽) (ref 9) are also shown for comparison.

one significant digit in the energy gap law parameters and hence extract an accurate value of $\beta_{el}$ for $S_2-S_1$ coupling in this system. Nevertheless, comparison of the values of $k_{nr}$ for Sn(IV)$Cl_2$TPP at an energy gap of $\Delta E(S_2-S_1) = 6875$ $cm^{-1}$ (a typical value for other tetraphenylmetalloporphyrins examined previously[9,10]) shows that the radiationless decay rate of the $S_2$ state of Sn(IV)$Cl_2$TPP is within a factor of 2 of that of MgTPP at the same energy gap, that is, only slightly faster than the weak coupling limit. Applying the empirical method used previously,[10] our best estimate of the electronic matrix element for $S_2-S_1$ coupling in Sn(IV)$Cl_2$TPP is therefore $\beta_{el} = 100$ $cm^{-1}$.

The temporal profiles of the $S_1$ population rise and decay were also measured by the fluorescence upconversion method in a more limited number of solvents. These measurements yield rather noisy data (cf., Figure 4) because the quantum yield of $S_1$ fluorescence is small (cf., Table 1) and because the oscillator strength of the $S_1-S_0$ transition is considerably smaller than that of the Soret transition. The upconverted photon count rate is therefore very low. Nevertheless, reasonable data could be obtained for the $S_1$ population risetime using a two-parameter fit as described above. The data obtained are also collected in Table 1. Note that the $S_1$ population rise times are all identical to the $S_2$ decay times within experimental error. This observation is consistent with those for MgTPP, ZnTPP, and other zinc porphyrins[9,10] with $S_2$ population decay times in the picosecond range and suggests that no longer-lived intermediate dark state is involved in the overall $S_2-S_1$ relaxation process of Sn(IV)$Cl_2$TPP.

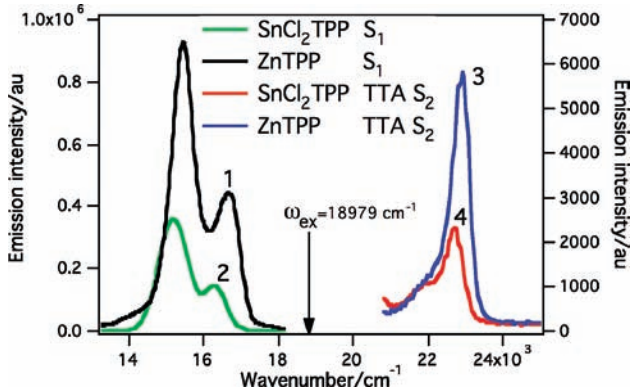


**Figure 6.** Prompt $S_1-S_0$ fluorescence (left-hand scale) of (1) ZnTPP and (2) Sn(IV)$Cl_2$TPP and TTA $S_2-S_0$ delayed fluorescence (right-hand scale) of (3) ZnTPP and (4) Sn(IV)$Cl_2$TPP in degassed benzene. The delayed $S_2$ fluorescence spectra were measured with different spectral slit widths, and the intensities displayed should be divided by $1.24 \times 10^2$ for ZnTPP and by $1.03 \times 10^4$ for Sn(IV)$Cl_2$TPP to account for differences (see text in Experimental Section). The ratio of the delayed fluorescence intensity of ZnTPP to that of Sn(IV)$Cl_2$TPP is 220.

The results of experiments to determine the efficiency of triplet−triplet annihilation of Sn(IV)$Cl_2$TPP as compared to ZnTPP in degassed benzene are shown in Figure 6. Solutions of these two metalloporphyrins were prepared with nearly identical absorbances at 532 nm, and their prompt $S_1-S_0$ and delayed $S_2-S_0$ emission spectra were taken under identical measurement conditions except for emission slit width. The known efficiency of TTA for ZnTPP in a noncoordinating solvent[12] can thus be used as a comparative standard for assessing the TTA efficiency in Sn(IV)$Cl_2$TPP. Note that the relative $S_2$ delayed fluorescence intensity of Sn(IV)$Cl_2$TPP is substantially lower than that of ZnTPP, indicating a lowered TTA efficiency in the former (vide infra).

## Discussion

The spectroscopic and photophysical data reported above for Sn(IV)$Cl_2$TPP now provide the basis for addressing open questions concerning the parameters that control the radiationless decay rates of the excited electronic states of the $d^0$ and $d^{10}$ metalated tetrapyrroles populated on one-photon excitation in their Soret absorption bands. We base our analysis on the understanding that the strong absorption feature in the violet region and its weaker satellite some 1300−1400 $cm^{-1}$ to the blue both belong to a single electronic transition,[23] $2(^1E_u)-1(^1A_{1g})$ in $D_{4h}$ symmetry, as described above.

We begin with more minor effects associated with the differences in the nature of the coordinated metals. In the four molecules of the MTPP series for which detailed data are now available, Mg(II) has a $d^0$ electron configuration, whereas Zn(II), Cd(II), and Sn(IV) are all $d^{10}$. Because solvent−solute dispersive interactions are important in these systems,[9,10] any significant contribution of the metal polarizability to the excited state relaxation processes should be revealed by comparisons among these four MTPP targets. However, no significant differences traceable to metal polarizability are found in the excited-state behavior of MgTPP, ZnTPP, and $SnCl_2$TPP. (Data for CdTPP are scant.[9]) Their $S_2-S_1$ energy spacings, which are controlled by the difference in excited state polarizabilities, are all similar in similar solvents. The gradients $g = |\partial(\Delta E)/\partial(f_1)|$ of plots such as Figure 3 are very similar,[9,10] and the small difference in the Sn(IV) compound is traceable to the presence of its covalently bonded axial ligands. Thus, there is no direct evidence that metal polarizability has any significant effect on the $S_2$ population decay dynamics of the $d^0$ and $d^{10}$ metalloporphyrins. This conclusion is reinforced by previous direct NMR measurements of the chemical shift tensors of the magnesium and zinc tetraphenylporphyrins, which are not significantly different despite the filled d shell in the latter.[29] Likewise, there is no correlation between excited-state photophysics and metal electronegativity.

Second, we consider the possible existence of multiple parallel $S_2$ population decay paths in these systems and how such additional decay channels might differ among the different $d^0$ and $d^{10}$ metalated species. TD-TFT calculations[30] reveal that there are several triplet states at energies lower than those of the $S_2$ states of MgTPP, ZnTPP, and CdTPP. Singlet−triplet intersystem crossing rates scale as the square of the interstate coupling energies, which in turn increase with the square of the metal's atomic number.[31] Therefore, differences among the overall $S_2$ radiationless decay rates of these molecules might be attributable to differences in their parallel $S_2-T_n$ ($n > 2$) intersystem crossing rates. Cd and Sn are both relatively heavy atoms, so the effects of spin−orbit coupling on the $S_2$ radiationless decay rates should be revealed when comparing $SnCl_2$TPP and CdTPP with MgTPP and ZnTPP. Indeed, the internal conversion efficiencies, $\eta_{S2S1}$, decrease in the order $\eta_{S2S1} = 1.00$ (MgTPP), 0.93 (ZnTPP), 0.86 ($SnCl_2$TPP), and 0.69 (CdTPP),[9] so intersystem crossing may contribute an increasing (small) fraction of the $S_2$ decay events in those porphyrins metalated with the heavier metals. However, comparing the $S_2$ population decay data obtained here with those obtained previously for MgTPP, ZnTPP, and CdTPP[9,10] reveals that the $S_2$ radiationless decay rate of CdTPP is the "odd man out" and is approximately a factor of 5 faster than that of $SnCl_2$TPP at the same electronic energy gap. The involvement of a parallel $S_2-T_n$ intersystem crossing decay route cannot account for this difference in rates because (i) the spin−orbit coupling constants for CdTPP and $SnCl_2$TPP will be similar, and (ii) in any case, net $S_2-S_1$ internal conversion accounts for by far the largest fraction of the $S_2$ radiationless decay events in both molecules (0.69 in CdTPP and 0.86 in $SnCl_2$TPP).[9] Although $S_2-T_n$ intersystem crossing may indeed account for a minor fraction of $S_2$ decay events, we nevertheless rule out differences in intersystem crossing rates as the source of the major differences in overall $S_2$ population decay rates in these four metalated tetraphenylporphyrins.

We now consider the more important effects of molecular symmetry, macrocycle rigidity, and surface displacement on the $S_2-S_1$ decay rates of these metalloporphyrins. We have previously shown[9,10] that in MgTPP the variation of the $S_2$ population decay rate with $S_2-S_1$ electronic energy spacing can be satisfactorily interpreted using the weak coupling case of radiationless transition theory, as developed from time-dependent perturbation theory. The data presented above now show that Sn(IV)$Cl_2$TPP and MgTPP behave similarly, with the former exhibiting a decay rate that is a factor of less than 2 larger than that of the latter at the same energy gap. However, the $S_2$ radiationless decay rates of CdTPP are much faster, and, although the $S_2-S_1$ decay rates of ZnTPP follow an energy gap law format, the gradient of that plot (cf., Figure 5) is larger than predicted by the weak coupling limit.[9,10] Thus, further analysis of the factors controlling these nonradiative rates is required. We start with the analytical expression developed by Englman and Jortner[28] for the weak coupling limit:

$$k_{nr} = \{\sqrt{2\pi C^2}/\hbar(\hbar\omega_M \Delta E)^{1/2}\} \exp\{-(\gamma/\hbar\omega_M)\Delta E\} \quad (1)$$

where

$$\gamma = \ln\{2\Delta E/\sum_M \hbar\omega_M \Delta_M^2\} - 1 \quad (2)$$

and $C$ is the interstate coupling energy, $\Delta E$ is the electronic energy gap between the two coupled states, $\hbar\omega_M$ is the wavenumber of the accepting vibrational mode in the lower state, $\Delta_M$ is the reduced displacement of the upper state surface relative to the lower one, and the summation is over all accepting modes. Previous work[10] has shown that the dominant accepting modes in $S_2-S_1$ radiationless decay in the $D_{4h}$ metalloporphyrins are the set of in-plane C−C and C−N stretching vibrations whose average frequency is ca. 1350 $cm^{-1}$, and which appear as the envelope that constitutes the weak (1−0) vibronic feature to the blue of the main Soret band in these molecules. There are about 30 such modes that contribute in *meso*-tetraarylmetalloporphyrins of $D_{4h}$ symmetry, so in such molecules we can replace the sum in eq 2 by multiplying its terms by the "degeneracy" $d_M \approx 30$.

Equations 1 and 2 also allow one to interpret those effects of surface displacement on $k_{nr}$ that are independent of the inverse exponential variation of the Franck−Condon factor with $\Delta E$ by finding $\Delta_M$ at constant $\Delta E$. Such displacements are potentially important in determining $S_2-S_1$ decay rates in the metalloporphyrins because the two coupled states are of the same electronic symmetry ($^1E_u$ in $D_{4h}$). Thus, among several similar metalloporphyrins, a progression from weak coupling ($S_2$ fully "nested" within $S_1$) to strong coupling[28] ("intersection" of the zero order $S_2$ and $S_1$ surfaces) is possible solely on the basis of variations in $\Delta_M$. In principle, the required $\Delta_M$ ($\equiv\Delta_{S2-S1}$) data can be obtained by difference from the Franck−Condon factors for the vibrational features in the Q and B absorption spectra, and we adopt such a procedure below.

In cases where the electronic transition is strongly allowed, such as the Soret band, measurement of the relative intensities of vibrational features corresponding to $\Delta v = 0, 1$ in the spectrum permits a direct calculation of the associated average Franck−Condon factors.[21] Here, we follow the analytical treatment developed by Siebrand[32] for the displaced, undistorted oscillator case, which is appropriate for the Soret band system. The small relative intensity of the (1−0) vibronic band envelope in the Soret system (Figure 1) is consistent with this approach. Thus, the Franck−Condon factors are given by:

$$F_{0v} = \frac{\delta^v}{v!} \exp(-\delta) \quad (3)$$

where $v$ is the quantum number of the vibration in the terminal state, and $\delta$ is a dimensionless parameter given by $\delta = K\Delta_M^2/2\hbar\omega$ for a harmonic oscillator of force constant $K$, displacement $\Delta_M$, and frequency $\hbar\omega$. The average values of $\delta = F_{01}/F_{00}$ are then obtained directly from the relative intensities of the (1−0) to (0−0) band envelopes in the Soret absorption system. The values of $\delta$ scale as $\Delta_M^2$ and can be used to determine the relative displacement of the upper state potential surface relative to that of the ground state. For the Soret band system of $Sn(IV)Cl_2TPP$, $\delta_S = 0.082$ averaged over several solvents, and this should be interpreted as an average associated with displacements along all of the $a_{1g}$ vibrational coordinates of the molecule. Similar calculations for the Soret band systems of MgTPP and ZnTPP reveal that the values of $\delta_S$ are similar for MgTPP, ZnTPP, and $Sn(IV)Cl_2TPP$, but are significantly larger for CdTPP. The data are collected in Table 2.

**TABLE 2: Parameters Describing Excited-State Displacements in Tetraphenylmetalloporphyrins[a]**

| compound | $(\varepsilon_{10}/\varepsilon_{00})_S$ | $\delta_S$ | $(\varepsilon_{20}/\varepsilon_{10})_Q$ | $(F_{02}/F_{01})_Q$ | $\delta_Q$ | $\Delta_{S2-S1}$[b] |
|---|---|---|---|---|---|---|
| MgTPP | 0.064 | 0.064 | 0.12 | 0.11 | 0.22 | 0.31 |
| ZnTPP | 0.070 | 0.070 | 0.15 | 0.13 | 0.26 | 0.35 |
| $Sn(IV)Cl_2TPP$ | 0.082 | 0.082 | 0.15 | 0.13 | 0.26 | 0.32 |
| CdTPP | 0.13 | 0.13 | 0.20 | 0.16 | 0.32 | 0.29 |

[a] Data for MgTPP, ZnTPP, and CdTPP are obtained from the spectra of ref 9. [b] Estimated error in $\Delta_{S2-S1}$ is ±10%.

Obtaining similar data from the Q-band spectra for the displacements of the $S_1$ potential surfaces is not as straightforward because this transition is quasi-forbidden[21] and the (1−0) band envelope contains large contributions to its intensity from vibronic coupling of the Q and B states by $a_{2g}$, $b_{1g}$, and $b_{2g}$ in-plane, nontotally symmetric vibrations (for $D_{4h}$ molecules), whereas the (0−0) band does not. However, if the small contribution to the (1−0) intensity from $a_{1g}$ vibrations is factored out (using eq 3 and values of $\delta_Q$ obtained as indicated below to obtain $I_{01}'$), then the ratio of the intensities of the (2−0) to the (1−0) vibrational envelopes in the Q-band system can be used to find $\delta_Q$ for the $S_1$ surface, that is, $I_{02}/I_{01}' = F_{02}/F_{01} = \delta_Q/2$.[32] The (2−0) band envelopes in the absorption spectra are weak and often not well resolved from the (1−0) band, but resolution of the spectrum into a sum of Gaussian features results in a reasonable measure of the relative intensities. The resulting values of $\delta_Q$ are displayed in Table 2. Note that the values of $\delta_Q$ are systematically larger than those of $\delta_S$, but that the two sets of values vary in the same sense and in the same order for the series MgTPP, ZnTPP, $Sn(IV)Cl_2TPP$, CdTPP. The dimensionless displacement of the $S_2$ surface relative to the $S_1$ surface, $\Delta_{S2-S1}$, then is obtained from the magnitude of the difference (cf., Supporting Information):

$$|\delta_S^{1/2} - \delta_Q^{1/2}| = 2^{-1/2}\Delta_{S2-S1} \quad (4)$$

The data are compiled in Table 2. Note that the values of $\Delta_{S2-S1}$ are similar for the three $D_{4h}$ metalloporphyrins despite the fact that the displacements of the individual excited-state surfaces are significantly different. These values are identical to those obtained previously from the energy gap law plot for MgTPP[9] (cf., Figure 5) in which it was assumed that the accepting modes are in-plane C−C and C−N stretches of average $\hbar\omega_M = 1350$ $cm^{-1}$ and of degeneracy $d_M \approx 30$. Note also that the value of $\Delta_{S2-S1}$ for CdTPP is the same as that for the other three tetraphenylmetalloporphyrins, despite the fact that the displacements of its individual $S_2$ and $S_1$ surfaces relative to the ground state are rather larger than the those of the others. The much faster $S_2$ decay rate for CdTPP and the steeper than predicted slope of the energy gap law plot for ZnTPP therefore cannot be rationalized on the basis of potential surface displacements.

Other factors must be responsible for the large differences in $S_2-S_1$ radiationless decay rates among these compounds, and we now directly examine the effect of molecular geometry. The $Sn^{4+}$ ion (radius, $r = 0.103$ nm) in $Sn(IV)Cl_2TPP$ is almost the same size as the $Zn^{2+}$ ion ($r = 0.107$ nm) in ZnTPP and the $Mg^{2+}$ ion ($r = 0.102$ nm) in MgTPP, but all three are smaller than the $Cd^{2+}$ ion ($r = 0.120$ nm) in CdTPP. (Note that these

ionic radii are all obtained from electron density contours[33] constructed from X-ray diffraction data; similar arguments can be made on the basis of the more traditionally accepted values of the ionic radii.) The most appropriate symmetry group for bare MgTPP and ZnTPP is $D_{4h}$, but, depending upon phase and solvation, both molecules can exhibit small deviations from this high symmetry,[34] an effect that is enhanced by strongly bound solvates such as water that tend to pull the metal atom out-of-plane.[35] On the other hand, Sn(IV)$Cl_2$TPP exhibits perfect $D_{4h}$ symmetry[15] and, with the two Cl atoms axially coordinated to the metal, is likely to be much less susceptible to deformation by specific solvation effects.

In contrast, the larger cadmium atom in CdTPP is permanently squeezed out-of-plane. Not only is its metalated macrocycle structure better described by the $C_{4v}$ point group, but it also exhibits significant flexibility leading to deviations from 4-fold symmetry.[36] Comparisons (vide infra) among MgTPP, ZnTPP, CdTPP, and Sn(IV)$Cl_2$TPP should therefore reveal the effects of molecular geometry and perhaps flexibility on their $S_2$ radiationless decay rates.

Considering the phenyl groups as point masses, there are 105 normal modes of vibration in the MTPP metalloporphyrins.[37] For the $D_{4h}$ molecules, 71 of these are in-plane vibrations, of which 35 are of gerade symmetry, that is, $\Gamma(\text{in-plane}) = 9a_{1g} + 8a_{2g} + 9b_{1g} + 9b_{2g} + 18e_u$. Only the 35 gerade vibrations can facilitate radiationless decay by coupling $S_2$ ($2^1E_u$) and $S_1$ ($1^1E_u$). In $C_{4v}$ molecules such as CdTPP, the two coupled electronic states are both of E symmetry, and vibrations of any symmetry can then couple the two states. Faster rates of radiationless decay must result. In principle, we should be able to use eqs 1 and 2 to estimate the effect on $k_{nr}$ of increasing the number of vibrations facilitating $S_2-S_1$ coupling in moving from a molecule of $D_{4h}$ symmetry such as Sn(IV)$Cl_2$TPP to one of $C_{4v}$ symmetry such as CdTPP. However, insufficient data are available to permit this.

Instead, we strengthen our argument by considering the photophysical behavior of other metalated tetrapyrroles whose symmetries are known to be lower than $D_{4h}$. The tetrapentafluorophenyl derivative of zinc porphyrin (ZnTPP($F_{20}$), of $S_4$ or "ruffled" symmetry) and the gallium and aluminum tripentafluorophenylcorroles (Al(tpfc)(py) and Ga(tpfc)(py) of approximate $C_{2v}$ symmetry) provide supporting data.[10,11] All three of these metalated tetrapyrroles have values of $\Delta E(S_2-S_1)$ similar to those of the MTPP series examined here, and all three also exhibit $S_2$ population decay primarily via $S_2-S_1$ internal conversion. However, all three exhibit $S_2$ population decay rates that are similar to that of CdTPP, that is, much faster than predicted by the weak coupling limit exemplified by MgTPP. Specifically, the ratios, $R$, of the rate constants for their $S_2$ population decay as compared to that of MgTPP ($R = 1.0$)[9] at the same energy gap (6875 $cm^{-1}$) are: $R = 5.8$ for ZnTPP($F_{20}$); $R = 4.8$ for Al(tpfc)(py); $R = 9.1$ for Ga(tpfc)(py), all in benzene at room temperature. This compares with $R = 8.8$ for CdTPP under the same conditions and vales of $R \leq 2$ for ZnTPP and Sn(IV)$Cl_2$TPP at the same energy gap. Small differences in the decay rates might be attributed to small differences in the interstate coupling constants ($C$ in eq 1). However, we conclude that molecular rigidity and high symmetry also provide a means of retarding $S_2-S_1$ radiationless decay in the $D_{4h}$ *meso*-phenyl-substituted tetrapyrroles by limiting the number of vibrations that can promote $S_2$ radiationless decay effectively. This conclusion is consonant with those made earlier regarding the differences in the spectroscopy and photophysics of the $S_1$ states of a larger set of planar, ruffled, and saddle-shaped metalloporphyrins.[38]

It is interesting to speculate that the slightly anomalous $S_2$ population decay behavior of ZnTPP (i.e., the larger than "expected" slope of its energy gap law plot, Figure 5) might also be traceable to its slightly more flexible macrocycle framework and the influence on the vibrational dynamics associated with specific solvation effects.[39] The effect of solvatochromism on the electronic energy gap, $\Delta E(S_2-S_1)$, and the resulting influence on the rate of $S_2-S_1$ radiationless decay have now been clearly established for several individual metalloporphyrins.[9,10] However, the influence of differences in specific solvation effects among different metalloporphyrins has not yet been elucidated. MgTPP tends to be preferentially axially coordinated by two solvent molecules in coordinating solvents such as pyridine and therefore maintains $D_{4h}$ symmetry even when considering solvate structures. On the other hand, ZnTPP tends to accept only one coordinating solvent molecule so that the overall symmetry of the dominant solvate is lower in ZnTPP than in MgTPP.[34,35] Such specific solvation effects should be absent in Sn(IV)$Cl_2$TPP where the two chlorine atoms occupy both axial coordination sites. It is therefore reasonable to suggest that the similar energy gap law behavior of MgTPP and Sn(IV)$Cl_2$TPP (cf., Figure 5) and the larger than expected gradient of this plot for ZnTPP may be traced to the differences in the specific solvation effects of these species.

Finally, we examine the effects of covalent axial ligation on the rates of TTA in these systems by comparing the $S_2$ yield resulting from $2T_1 \rightarrow S_2 + S_0$ annihilation in Sn(IV)$Cl_2$TPP with that in ZnTPP, both in noncoordinating solvents (benzene or toluene) at room temperature. We have previously shown[12] that the relative intensities of $S_2 \rightarrow S_0$ delayed fluorescence produced by this TTA process, when initiated by cw excitation in the Q-band, can be used as a metric for the effects of axial coordination by solvent. Thus, for ZnTPP, the intensity of $S_2$ delayed fluorescence is reduced by a factor of about 20 in pyridine (coordinating) as compared to benzene (noncoordinating) under otherwise identical conditions. These relative $S_2$ fluorescence intensities are quantitatively consistent with the short-range, electron exchange (Dexter) mechanism of TTA.

A steady-state analysis of the mechanism of TTA (cf., Supporting Information) results in the following relationship for $R_{TTA}$, the ratio of the intensity of $S_2$ delayed fluorescence produced in Sn(IV)$Cl_2$TPP to that in ZnTPP in the same noncoordinating solvent (benzene) under identical conditions.

$$R_{TTA} = \frac{k_{TTA}^{Sn}}{k_{TTA}^{Zn}} = \left(\frac{I_{dfS2}^{Sn}}{I_{dfS2}^{Zn}}\right)\left(\frac{\phi_{fS2}^{Zn}}{\phi_{fS2}^{Sn}}\right)\left(\frac{\tau_{T1}^{Zn}}{\tau_{T1}^{Sn}} \cdot \frac{\phi_{iSC,S1}^{Zn}}{\phi_{isc,S1}^{Sn}} \cdot \frac{I_a^{Zn}}{I_a^{Sn}}\right)^2 \quad (5)$$

We have measured the intensities of delayed $S_2$ fluorescence ($I_{dfS2}$, Figure 6) under conditions where the absorbed intensities at 532 nm, $I_a$, are almost identical in these two systems and have measured the quantum yields of prompt $S_2$ fluorescence ($\phi_{fS2}$, Table 1). The quantum efficiencies of $S_1-T_1$ intersystem crossing, $\phi_{isc,S1}$, have been measured previously by others[6] and are large and similar, so the only unknowns in eq 5 are the unquenched lifetimes of the triplet states, $\tau_{T1}$, of the two metalloporphyrins under the conditions of the TTA experiment. If we use data for the triplet lifetimes previously measured in glassy matrices[6] at 77 K, $\tau_{T1} = 26$ ms for ZnTPP, and $\tau_{T1} = 11.3$ ms for Sn(IV)$Cl_2$TPP, and assume that the ratio of these unquenched triplet lifetimes is the same under the conditions

of our TTA measurements, we obtain $R_{TTA} = 4.6 \times 10^{-3}$. This value can be related to the increase in the average distance between the two annihilating triplets, $\Delta d$, caused by the presence of the axial ligands on the Sn(IV)$Cl_2$TPP using (cf., Supporting Information):

$$R_{TTA} = \exp\{-2\Delta d/0.48\} \quad (6)$$

The difference is $\Delta d = 0.61$ nm, which is between 3 and 4 times the van der Waals radius of a chloride ion. This datum suggests that the distance of closest approach of the two triplets during annihilation is greatly increased in Sn(IV)$Cl_2$TPP relative to MgTPP or ZnTPP due to the shielding effect of the two axial chloride ligands. Accurate measurements of the triplet lifetimes under the conditions of the TTA experiment will be needed to confirm this suggestion.

## Conclusions

Measurements of the $S_2$ population decay rates and triplet−triplet annihilation efficiencies of Sn(IV)$Cl_2$TPP in fluid solutions have been made for the first time using its weak $S_2-S_0$ fluorescence as a metric. The resulting detailed description of the excited state photophysics of Sn(IV)$Cl_2$TPP allows comparisons to be made between the behavior of this rigid, $D_{4h}$ axially coordinated molecule and axially uncoordinated tetrapyrroles of greater flexibility and lower symmetry. The following conclusions have been drawn and provide the basis for more fully understanding the factors that control the radiationless decay rates of the Soret-excited metalated tetrapyrroles.

(i) $S_2-S_1$ internal conversion is the major $S_2$ population decay path for Sn(IV)$Cl_2$TPP, as it is for the $S_2$ states of all other $d^0$ and $d^{10}$ metalated tetrapyrroles. $S_2-T_n$ ($n > 2$) intersystem crossing can account for only a small fraction of the $S_2$ relaxation events, irrespective of the "heavy atom" effect.

(ii) The $S_2$ state of Sn(IV)$Cl_2$TPP exhibits $S_2-S_1$ relaxation rates that are only slightly faster than those exhibited by MgTPP and the weak coupling limit. The $S_2-S_1$ interstate coupling energy is of the order of 100 $cm^{-1}$.

(iii) Differences in $S_2-S_1$ radiationless decay rates among the series MTPP (M = Mg, Zn, Cd, $SnCl_2$) cannot be traced to differences in the displacements of the $S_2$ and $S_1$ potential surfaces even though the displacements of the excited-state surfaces relative to the ground state differ and the Stokes shifts increase in the order Mg ≈ $SnCl_2$ < Zn < Cd.

(iv) The most likely source of the large differences in $S_2-S_1$ radiationless decay rates between CdTPP and Sn(IV)$Cl_2$TPP is the lower symmetry of the former (near $C_{4v}$), which permits a much larger number of vibrations to participate in $S_2-S_1$ vibronic coupling.

(v) Triplet−triplet annihilation of the type $2T_1 \rightarrow S_2 + S_0$ has been observed in Sn(IV)$Cl_2$TPP for the first time, but is of substantially lower efficiency than that found in ZnTPP in noncoordinating solvents because of the shorter triplet lifetime of Sn(IV)$Cl_2$TPP and the shielding effects of its axial Cl ligands, which tend to block the short-range interaction needed for Dexter energy transfer.

The detailed picture of the photophysics of Soret-excited Sn(IV))$Cl_2$TPP presented here, together with the results described in previous papers in this series,[9,10,11a] provides a more comprehensive picture of the factors controlling the rates of radiationless decay of this important class of compounds. Metalated macrocycle symmetry and flexibility play a crucial role in determining the magnitude of the deviation (increase) in $S_2-S_1$ relaxation rate from the lower limit established by weak vibronic coupling in rigid molecules of $D_{4h}$ symmetry.

**Acknowledgment.** We gratefully acknowledge the Natural Sciences and Engineering Research Council of Canada and the Canada Foundation for Innovation for financial support of this research. Dr. Sophie Brunet, Saskatchewan Structural Sciences Centre, is acknowledged for laser training and technical assistance. We are also grateful to Dr. Hans-Christian Becker, Uppsala University, for providing the fitting program.

**Supporting Information Available:** Derivations of eqs 4−6. This material is available free of charge via the Internet at http://pubs.acs.org.

## References and Notes

(1) (a) Dolphin, D., Ed. *The Porphyrins*; Academic Press: New York, 1978; Vol. VI. (b) Kadish, K. K.; Smith, K. M.; Guilard, R. *The Porphyrin Handbook*; Academic Press: San Diego, CA, 2000.

(2) Brinas, R. P.; Troxler, T.; Hochstrasser, R. M.; Vinogradov, S. A. *J. Am. Chem. Soc.* **2005**, *127*, 1530.

(3) (a) Szacillowski, K.; Macyk, W.; Drzewiecka-Matuszek, A.; Brindell, M.; Stochel, G. *Chem. Rev.* **2005**, *105*, 2647. (b) Donzello, M. P.; Ercolani, C.; Stuzhin, P. A. *Coord. Chem. Rev.* **2006**, *250*, 1530.

(4) (a) Lee, T.-H.; Gonzalez, J. I.; Zheng, J.; Dickson, R. M. *Acc. Chem. Res.* **2005**, *38*, 534. (b) Perez-Inestrosa, E.; Montenegro, J.-M.; Collado, D.; Suau, R.; Casado, J. *J. Phys. Chem. C* **2007**, *111*, 6904. (c) Langford, S. J.; Yann, T. *J. Am. Chem. Soc.* **2003**, *125*, 11198. (d) Remacle, F.; Speiser, S.; Levine, R. D. *J. Phys. Chem. A* **2001**, *105*, 5589. (e) Yeow, E. K. L.; Steer, R. P. *Chem. Phys. Lett.* **2003**, *377*, 391.

(5) (a) Nakano, A.; Osuka, A.; Yamazaki, T.; Nishimura, Y.; Akimoto, S.; Yamazaki, I.; Itaya, A.; Murakami, M.; Miyasaka, H. *Chem.-Eur. J.* **2001**, *7*, 3134. (b) Wagner, R. W.; Johnson, T. E.; Lindsey, J. S. *J. Am. Chem. Soc.* **1996**, *118*, 11166.

(6) For a review, see: Takagi, S.; Inoue, H. In *Molecular and Supramolecular Photochemistry*; Ramamurthy, V., Schanze, K. S., Eds.; Marcel Dekker: New York, 2000; Vol. 5, p 215.

(7) For reviews, see: (a) Tripathy, U.; Steer, R. P. *J. Porphyrins Phthalocyanines* **2007**, *11*, 228. (b) Burdzinski, G.; Kubicki, J.; Maciejewski, A.; Steer, R. P.; Velate, S.; Yeow, E. K. L. In *Organic Photochemistry and Photophysics*; Ramamurthy, V., Schantze, K. S., Eds.; Marcel Dekker: New York, 2005; Vol. 14, p 1.

(8) (a) Baluschev, S.; Yakutkin, V.; Miteva, T.; Wegner, G.; Roberts, T.; Nelles, G.; Yasuda, A.; Chernov, S.; Aleshchenkov, S.; Chelprakov, A. *New J. Phys.* **2008**, *10*, 013007. (b) Baluschev, S.; Yakutkin, V.; Wegner, G.; Miteva, T.; Nelles, G.; Yasuda, A.; Chernov, S.; Aleshchenkov, S.; Chelprakov, A. *Appl. Phys. Lett.* **2007**, *90*, 181103. (c) Baluschev, S.; Yakutkin, V.; Miteva, T.; Avlasevich, Y.; Chernov, S.; Aleshchenkov, S.; Nelles, G.; Cheprakov, A.; Yasuda, A.; Müllen, K.; Wegner, G. *Angew. Chem., Int. Ed.* **2007**, *46*, 7693. (d) Baluschev, S.; Yakutkin, V.; Wegner, G.; Minch, B.; Miteva, T.; Nelles, G.; Yasuda, A. *J. Appl. Phys.* **2007**, *101*, 023101. (e) Baluschev, S.; Miteva, T.; Yakutkin, V.; Nelles, G.; Yasuda, A.; Wegner, G. *Phys. Rev. Lett.* **2006**, *97*, 143903. (f) Baluschev, S.; Keivanidis, P. E.; Wegner, G.; Jacob, J.; Grimsdale, A. C.; Müllen, K.; Miteva, T.; Yasuda, A.; Nelles, G. *Appl. Phys. Lett.* **2005**, *86*, 061904. (g) Baluschev, S.; Jacob, J.; Avlasevich, Y. S.; Keivanidis, P. E.; Miteva, T.; Yasuda, A.; Nelles, G.; Grimsdale, A. C.; Müllen, K.; Wegner, G. *ChemPhysChem* **2005**, *6*, 1250. (h) Baluschev, S.; Yu, F.; Miteva, T.; Ahl, S.; Yasuda, A.; Nelles, G.; Knoll, W.; Wegner, G. *Nano Lett.* **2005**, *5*, 2482. (i) Singh-Rachford, T. N.; Castellano, F. N. *Inorg. Chem.* **2009**, *48*, 2541. (j) Singh-Rachford, T. N.; Castellano, F. N. *J. Phys. Chem. A* **2008**, *112*, 3550. (k) Singh-Rachford, T. N.; Islangulov, R. R.; Castellano, F. N. *J. Phys. Chem. A* **2008**, *112*, 3906. (l) Islangulov, R. R.; Lott, J.; Weder, C.; Castellano, F. N. *J. Am. Chem. Soc.* **2007**, *129*, 12652. (m) Islangulov, R. R.; Castellano, F. N. *Angew. Chem., Int. Ed.* **2006**, *45*, 5957. (n) Zhao, W.; Castellano, F. N. *J. Phys. Chem. A* **2006**, *110*, 11440. (o) Islangulov, R. R.; Koslov, D. V.; Castellano, F. N. *Chem. Commun.* **2005**, 3776. (p) Monguzzi, A.; Tubino, R.; Meinardi, F. *Phys. Rev. B* **2008**, *77*, 155122. (q) Monguzzi, A.; Tubino, R.; Meinardi, F. *J. Phys. Chem. A* **2009**, *113*, 1171.

(9) Tripathy, U.; Kowalska, D.; Liu, X.; Velate, S.; Steer, R. P. *J. Phys. Chem. A* **2008**, *112*, 5824.

(10) Liu, X.; Tripathy, U.; Bhosale, S. V.; Langford, S. J.; Steer, R. P. *J. Phys. Chem. A* **2008**, *112*, 8986.

(11) (a) Liu, X.; Mahammed, A.; Tripathy, U.; Gross, Z.; Steer, R. P. *Chem. Phys. Lett.* **2008**, *459*, 113. (b) Kowalska, D.; Liu, X.; Tripathy, U.; Mahammed, A.; Gross, Z.; Hirayama, S.; Steer, R. P. *Inorg. Chem.* **2009**, *48*, 2670.

(12) Sugunan, S. K.; Tripathy, U.; Brunet, S. M. K.; Paige, M. F.; Steer, R. P. *J. Phys. Chem. A* **2009**, *113*, 8548.
(13) O'Brien, J. A.; Rallabandi, S.; Tripathy, U.; Paige, M. F.; Steer, R. P. *Chem. Phys. Lett.* **2009**, *475*, 220.
(14) Arnold, D. P.; Blok, J. *Coord. Chem. Rev.* **2004**, *248*, 299.
(15) Collins, D. M.; Scheidt, W. R.; Hoard, J. L. *J. Am. Chem. Soc.* **1972**, *94*, 6689.
(16) Debaig-Valade, C.; Bagno, O.; Pommier, J. C.; Joussot-Dubien, J. *Photochem. Photobiol.* **1981**, *33*, 899.
(17) Asadi, M.; Mohammadi, K.; Zebardasti, A. *Helv. Chim. Acta* **2002**, *85*, 2975.
(18) (a) Lukaszewicz, A.; Karolczak, J.; Kowalska, D.; Maciejewski, A.; Ziolek, M.; Steer, R. P. *Chem. Phys.* **2007**, *331*, 359. (b) Karolczak, J.; Kowalska, D.; Lukaszewicz, A.; Maciejewski, A.; Steer, R. P. *J. Phys. Chem. A* **2004**, *108*, 4570.
(19) (a) Gouterman, M.; Schwarz, F. P.; Smith, P. D.; Dolphin, D. *J. Chem. Phys.* **1973**, *59*, 676. (b) Gouterman, M.; Howell, D. B. *J. Chem. Phys.* **1974**, *61*, 3491.
(20) One previous report of Soret band emission is in error: Jang, J. H.; Hee, J. K.; Kim, C. H.; Joo, T.; Cho, D. W.; Yoon, M. *Bull. Korean Chem. Soc.* **2007**, *28*, 1967.
(21) Gouterman, M. *J. Chem. Phys.* **1959**, *30*, 1139.
(22) (a) Peralta, G. A.; Seth, M.; Ziegler, T. *Inorg. Chem.* **2007**, *46*, 9111. (b) For a review, see: Baerends, E. J.; Riccardi, G.; Rosa, A.; van Ginsberg, S. J. *Coord. Chem. Rev.* **2002**, *230*, 5.
(23) Solheim, H.; Ruud, K.; Coriani, S.; Norman, P. *J. Phys. Chem. A* **2008**, *112*, 9615.
(24) Strickler, S. J.; Berg, R. A. *J. Chem. Phys.* **1962**, *37*, 814.
(25) Gouterman, M. *J. Chem. Phys.* **1973**, *59*, 676.
(26) Grigg, R. *J. Chem. Soc., Chem. Commun.* **1992**, 1298.
(27) Tétreault, N.; Muthyala, R. S.; Liu, R. S. H.; Steer, R. P. *J. Phys. Chem. A* **1999**, *103*, 2524.
(28) Englman, R.; Jortner, J. *Mol. Phys.* **1970**, *18*, 145.
(29) Strohmeier, M.; Orendt, A. M.; Facelli, J. C.; Solum, M. S.; Pugmire, R. J.; Parry, R. W.; Grant, D. M. *J. Am. Chem. Soc.* **1997**, *119*, 7114.
(30) Liu, X.; Yeow, E. K. Y.; Velate, S.; Steer, R. P. *Phys. Chem. Chem. Phys.* **2006**, *8*, 1298.
(31) McGlynn, S. P.; Azumi, T.; Kinoshita, M. *Molecular Spectroscopy of the Triplet State*; Prentice-Hall: Englewood Cliffs, NJ, 1969.
(32) Siebrand, W. *J. Chem. Phys.* **1967**, *46*, 440.
(33) (a) Johnson, O. *Inorg. Chem.* **1973**, *12*, 780. (b) Johnson, O. *Chem. Scr.* **1975**, *7*, 5.
(34) (a) Timkovitch, R.; Tulinsky, A. *J. Am. Chem. Soc.* **1969**, *91*, 4430. (b) Wu, G.; Wong, A.; Wang, S. *Can. J. Chem.* **2003**, *81*, 275. (c) Scheidt, W. R.; Kastner, M. E.; Hatano, K. *Inorg. Chem.* **1978**, *17*, 706. (d) Scheidt, W. R.; Mondal, J. U.; Eigenbrot, C. W.; Alder, A.; Radonovitch, L. J.; Hoard, J. L. *Inorg. Chem.* **1986**, *25*, 795.
(35) (a) Golder, A. J.; Povey, D. C.; Silver, J.; Jassim, Q. A. A. *Acta Crystallogr.* **1990**, *C46*, 1210. (b) McKee, V.; Rodley, G. A. *Inorg. Chim. Acta* **1988**, *151*, 233.
(36) (a) Rodesiler, P. F.; Griffith, E. H.; Ellis, P. D.; Amma, E. L. *J. Chem. Soc., Chem. Commun* **1980**, 492. (b) Hazell, A. *Acta Crystallogr.* **1986**, *C42*, 296.
(37) Stein, P.; Ulman, A.; Spiro, T. G. *J. Phys. Chem.* **1984**, *88*, 369.
(38) (a) Irvine, M. P.; Harrison, R. J.; Strahand, M. A.; Beddard, G. S. *Ber. Bunsen-Ges. Phys. Chem.* **1985**, *89*, 226. (b) Rodriguez, J.; Kirmaier, C.; Holten, D. *J. Am. Chem. Soc.* **1989**, *111*, 6500. (c) Chirvony, V. S.; van Hoek, A.; Galievsky, V. A.; Sazanovitch, I. V.; Schaafsma, T. J.; Holten, D. *J. Phys. Chem. A* **2000**, *104*, 9909. (d) Retsek, J. L.; Gentemann, S.; Medforth, C. J.; Smith, K. M.; Chirvony, V. S.; Fajer, J.; Holten, D. *J. Phys. Chem. B* **2000**, *104*, 6690. (e) Smirnov, V. V.; Woller, E. K.; Tatman, D.; DiMagno, G. *Inorg. Chem.* **2001**, *40*, 2614. (f) Chen, Y.; Zhang, B.; Chen, J.-G.; Huang, D.-Y. *Spectrochim. Acta, Part A* **2001**, *57*, 2451. (g) Azhena, E. G.; Serra, A. C.; Pineiro, M.; Pereira, M. M.; de Melo, J. S.; Arnaut, L. G.; Formosinho, S. J.; Rocha Gonsalves, A. M. d'A. *Chem. Phys.* **2002**, *280*, 177. (h) Rogers, J. E.; Nguyen, K. A.; Hufnagle, D. C.; McLean, D. G.; Su, W.; Gossett, K. M.; Burke, A. R.; Vinogradov, S. A.; Pachter, R.; Fleitz, P. A. *J. Phys. Chem. A* **2003**, *107*, 11331.
(39) Nappa, M.; Valentine, J. S. *J. Am. Chem. Soc.* **1978**, *100*, 5075.

JP906966H